

Article

Energy Balance, Microclimate, and Crop Evapotranspiration of Winter Wheat (*Triticum aestivum* L.) under Sprinkler Irrigation

Xiaopei Tang ¹, Haijun Liu ^{1,*} , Li Yang ¹, Lun Li ¹ and Jie Chang ²

¹ Beijing Key Laboratory of Urban Hydrological Cycle and Sponge City Technology, College of Water Sciences, Beijing Normal University, Beijing 100875, China; tangxiaopei@mail.bnu.edu.cn (X.T.); 201921470027@mail.bnu.edu.cn (L.Y.); 202021470012@mail.bnu.edu.cn (L.L.)

² School of Water Conservancy and Environment, Zhengzhou University, Zhengzhou 450001, China; changjie@gs.zzu.edu.cn

* Correspondence: shanxiljh@bnu.edu.cn; Tel.: +86-13-681-334-108

Abstract: Understanding the impact of sprinkler irrigation on field energy balance, microclimate, and crop evapotranspiration is of great importance for optimizing irrigation scheduling and enhancing crop growth. In this study, the microclimate variables, energy, and water flux were measured using an eddy covariance system during four wheat (*Triticum aestivum* L.) growing seasons in a sprinkler-irrigated field of North China Plain. The variation patterns of microclimate, energy balance (net solar radiation R_n , soil heat flux G , latent heat LE , and sensible heat H) and crop evapotranspiration (ET) were analyzed during and after sprinkler irrigation events. A novel quantitative model using a stepwise regression method was developed to predict the change in microclimate after sprinkler irrigation by considering irrigation, weather, meteorology, and crop traits. The results showed that the reflectance rate of the wheat canopy decreased by 0.01, and the daily LE/R_n increased by 0.19–0.23 in the 1–3 days after sprinkler irrigation with 40–50 mm water, which finally resulted in crop ET increased by 1.8–4.7 mm during irrigation interval, and seasonal total ET could increase by 9–24 mm when five normal sprinkler irrigations were implemented in a wheat season. The mean daily H/R_n decreased by 0.06–0.17, indicating weak energy exchange between canopy and environment. The measured daily minimum (T_{min}), maximum temperatures (T_{max}) and daily mean vapor pressure deficit (VPD) decreased by approximately 0.8 °C, 0.9 °C, and 0.25 kPa, respectively, and daily mean relative humidity increased by approximately 7.5% on the first 3 days after sprinkler irrigation; and these changes decreased and were negligible on the 5th–7th days. The decreases in daily T_{min} , T_{max} , and mean VPD after sprinkler irrigation could change more under higher irrigation amounts and sunny days with a larger crop leaf area index based on the fitted models.

Keywords: sprinkler irrigation; microclimate; evapotranspiration; water fluxes; energy balance



Citation: Tang, X.; Liu, H.; Yang, L.; Li, L.; Chang, J. Energy Balance, Microclimate, and Crop Evapotranspiration of Winter Wheat (*Triticum aestivum* L.) under Sprinkler Irrigation. *Agriculture* **2022**, *12*, 953. <https://doi.org/10.3390/agriculture12070953>

Academic Editors: Jiandong Wang and Yanqun Zhang

Received: 26 May 2022

Accepted: 28 June 2022

Published: 30 June 2022

Publisher's Note: MDPI stays neutral with regard to jurisdictional claims in published maps and institutional affiliations.



Copyright: © 2022 by the authors. Licensee MDPI, Basel, Switzerland. This article is an open access article distributed under the terms and conditions of the Creative Commons Attribution (CC BY) license (<https://creativecommons.org/licenses/by/4.0/>).

1. Introduction

Irrigation, as an important anthropogenic activity, plays a critical role in increasing crop yields [1]. Wang et al. [2] reported that irrigation can increase yield by 34% for wheat and 22% for maize at the global scale. However, irrigation can also affect the hydrological cycle between land and atmosphere, which further affects the regional climate as well as the microclimate [3–5]. Irrigation can cool the land surface and increase air humidity in irrigation areas, as found in America [6], China [7,8], and India [9]. Because field microclimate directly influence crop growth, understanding the impact of irrigation on field microclimate could help improve crop growth and irrigation management [10–12].

Sprinkler irrigation is one of the main irrigation methods in the world because of its water saving and enhanced food productivity potential [11,13,14]. Based on the data of the International Commission on Irrigation and Drainage, sprinkler-irrigated areas account for 43% and 10% of the total irrigated area in developed and developing countries, respectively [15]. Because of the water evaporation from the droplets and canopy interception

during sprinkler irrigation, the water and heat balance in the field are modified, eventually leading to microclimate changes. By spraying 2–6 mm of water at 12:00 and 18:00 in a jujube (*Ziziphus jujube* Mill.) orchard at the flowering to fruit set stage, the mean daily canopy temperature during sprinkler irrigation events decreases between 1 and 3 °C, the mean daily relative humidity (RH) increases between 11 and 17%, and the mean daily vapor pressure deficit (VPD) decreases from 3 to 2 kPa [12]. The temperature at the top of the canopy is reduced by 1.1–1.6 °C after mist spraying 1 mm water at the flowering stage of rice (*Oryza sativa* L.), and this cooling effect lasts for approximately 2 h [11]. Compared with surface irrigation in the winter wheat field, daytime sprinkler irrigation with 50 mm water results in 1.1–2.9 °C lower air temperature and 2.8–4.0 kPa lower VPD at a 1 m height above the ground surface during the daytime and correspondingly 0.5–0.6 °C and 1.1–2.2 kPa during the nighttime [16]. Due to the cooling effect, sprinkling 1.0–1.5 mm water under dry-hot wind conditions is recommended to mitigate the high temperature effects on crops [17].

Due to the different irrigation systems, irrigation water amounts, climatic environments, and crop characteristics, the change extents of field microclimate under sprinkler irrigation differ in previous studies. For example, at the flowering to fruit set stage of jujube, spraying 6 mm water every day causes greater microclimate changes and improves photosynthetic capacity than those under 4 and 2 mm water [12]. Sprinkling on drier and warmer days has a greater impact on field microclimate and maize (*Zea mays*, L.) transpiration rate changes [18]. Owing to the higher stem and larger leaf area in maize than that in soybean (*Glycine max* [L.] Merr.), the microclimate change is more obvious and lasts for longer periods in maize fields [6]. To date, studies have mostly focused on changes in field microclimate during and/or a short time (a few hours) after sprinkler irrigation, and few have considered the differences in irrigation conditions (for example, irrigation amount), climatic environments, and crop characteristics and have not quantified long-duration field microclimatic changes after sprinkler irrigation.

Sprinkler irrigation modifies the energy and water flux among the atmosphere, crop, and soil surface. After mist spraying 1 mm water at noon in the period of flowering, the latent heat at the top of rice canopy increases by 53.6–61.8 W m⁻² and sensible heat decreases by 28.6–33.1 W m⁻² [11]. The evaporation of cotton canopy during sprinkler irrigation is 1.6 times higher than the dry canopy evaporation [19]. These changes in energy and water flux are the main reasons for microclimate variations in sprinkler-irrigated fields. However, few studies focus on energy balance and crop evapotranspiration changes over a long time after sprinkler irrigation, which impedes the full evaluation of sprinkler irrigation on field microclimate, crop growth, and water use efficiency.

The North China Plain (NCP) produces approximately 59% of China's total wheat (*Triticum aestivum* L.) and is a key base for high-quality wheat production in China [20]. However, precipitation in this region is very scarce, and cannot meet the water requirements of winter wheat [21]. To ensure the stability of and increase in wheat yield, irrigation of 200–300 mm is required every year [22,23]. Additionally, water shortage is critical in NCP. The amount of water resources used per capita in the NCP is 137 m³, which is 8% of the mean for China [20] and 3% of the global mean [24]. Recently, the groundwater level has declined at a rate of 1.35 m y⁻¹ because of agricultural irrigation [25]. Consequently, water-saving and efficient irrigation are key to solving the contradiction between water shortages and grain production in this region. Sprinkler irrigation, as a water-saving and highly water-use-efficient irrigation method, has been popularized in the NCP [26]. The total area of sprinkler-irrigated fields in the NCP is more than 0.67 million hectares, accounting for approximately 16% of the total sprinkler-irrigated area in China [27]. A deep understanding of microclimate change patterns, crop evapotranspiration, and energy balance in sprinkler-irrigated fields can benefit the evaluation of water use efficiency, crop production, and water resource management under sprinkler irrigation in the NCP as well as other regions with water shortage problems.

The objectives of this study were to (1) analyze the impact of sprinkler irrigation on field microclimate at different growth stages of winter wheat with different irrigation amounts, (2) explore the energy partitioning and crop evapotranspiration characteristics during and after sprinkler irrigation, and (3) establish a quantitative model to estimate field microclimate changes in winter wheat fields under sprinkler irrigation in the NCP.

2. Materials and Methods

2.1. Experimental Site

The experimental site was located in Ningjin County, Xingtai City, Hebei Province in the midwest NCP (Figure 1A) (The boundary of the North China Plain is derived from Zhang and Fei [28]), and has a typical temperate continental monsoon climate [29]. Precipitation in this region is concentrated between July and September, which accounted for approximately 70% of the annual amount. This climate determined the local predominant planting pattern of the winter wheat–summer maize double cropping system. Winter wheat was mostly sown in October and harvested in mid-June. In the wheat season, the average temperature was 7.9 °C, sunshine duration was 1632 h, and precipitation was 130 mm (1982–2018). A field experiment was carried out at Dacaozhuang Seed Experimental Station in the southwest of Ningjin County (37°30′ N latitude, 114°56′ E longitude, 26 m altitude), Hebei Province in the NCP (Figure 1B). Around the experimental field, there was approximately 4000 ha of farmland, all of which has been irrigated with sprinkler irrigation systems since the 1970s. The main soil texture of the topsoil (0–60 cm) was silty loam, consisting of 11% clay, 63% silt, and 26% sand. The soil field capacity and bulk density were $0.36 \text{ cm}^{-3} \text{ cm}^{-3}$ and 1.45 g cm^{-3} , respectively. A meteorological station, Station B (Figure 1B), was located in the Midwest of Ningjin County (37°38′ N latitude, 114°55′ E longitude, 30.1 m altitude), approximately 15 km away from Station A. About 10 cm height grass was planted inside Station B, and the surrounding was open and flat. Station B was a Chinese national basic meteorological station, and the measured data were the standard meteorological data published by Ningjin County Meteorological Bureau, which were generally used to guide the crops production for local farmers.

2.2. Experimental Design

The standard data measured at Station B of the national basic meteorological station, which was not affected by irrigation, crop, or other management factors [30], were treated as the non-irrigation treatment, while the data of winter wheat field under sprinkler irrigation at Station A were treated as the sprinkler irrigation treatment. At Station A, the field experiment was conducted during the 2017–2021 winter wheat growing season in a plot of 200 m × 60 m. A widely grown winter wheat variety in the study region, Yingbo 700, was sown on approximately 20 October and harvested on 10 June in the next year. The planting density was approximately 3.75 million seedlings ha^{-1} , and the row spacing was 15 cm. In each wheat season, before sowing, 40 kg N ha^{-1} , 90 kg $\text{P}_2\text{O}_5 \text{ ha}^{-1}$, and 60 kg $\text{K}_2\text{O} \text{ ha}^{-1}$ were applied as base fertilizers, and then urea (53 kg N ha^{-1} for each time) was completely dissolved in a fertilization device and applied as three topdressings together with irrigation water at the greening stage, jointing stage, and milking stage. A semifixed sprinkler irrigation system was used for irrigation. The sprinkler model was a PXS20-D (Tonghua Zhenyu Sprinkler Irrigation Equipment Factory, Zhenzhou, China), with a wetted radius of 18 m and a flow rate of $2.16 \text{ m}^3 \text{ h}^{-1}$ under 0.25 MPa working pressure. The spacings between both sprinklers and laterals were 18 m. The in situ measured water distribution coefficient calculated using the Christian method [31] was 0.84. The wheat in each season was irrigated after sowing and before overwintering. After wheat was regreened in March, the irrigation schedule was determined by the evaporation of a 20 cm pan. The irrigation amount each time was 0.65 times the difference between the cumulative evaporation amount of the 20 cm pan and precipitation during the two irrigation intervals [32]. In general, the water amount per sprinkler irrigation event was 20–50 mm, and the intervals were 10–14 days. The detailed irrigation schedule after regreening is shown in Table 1.

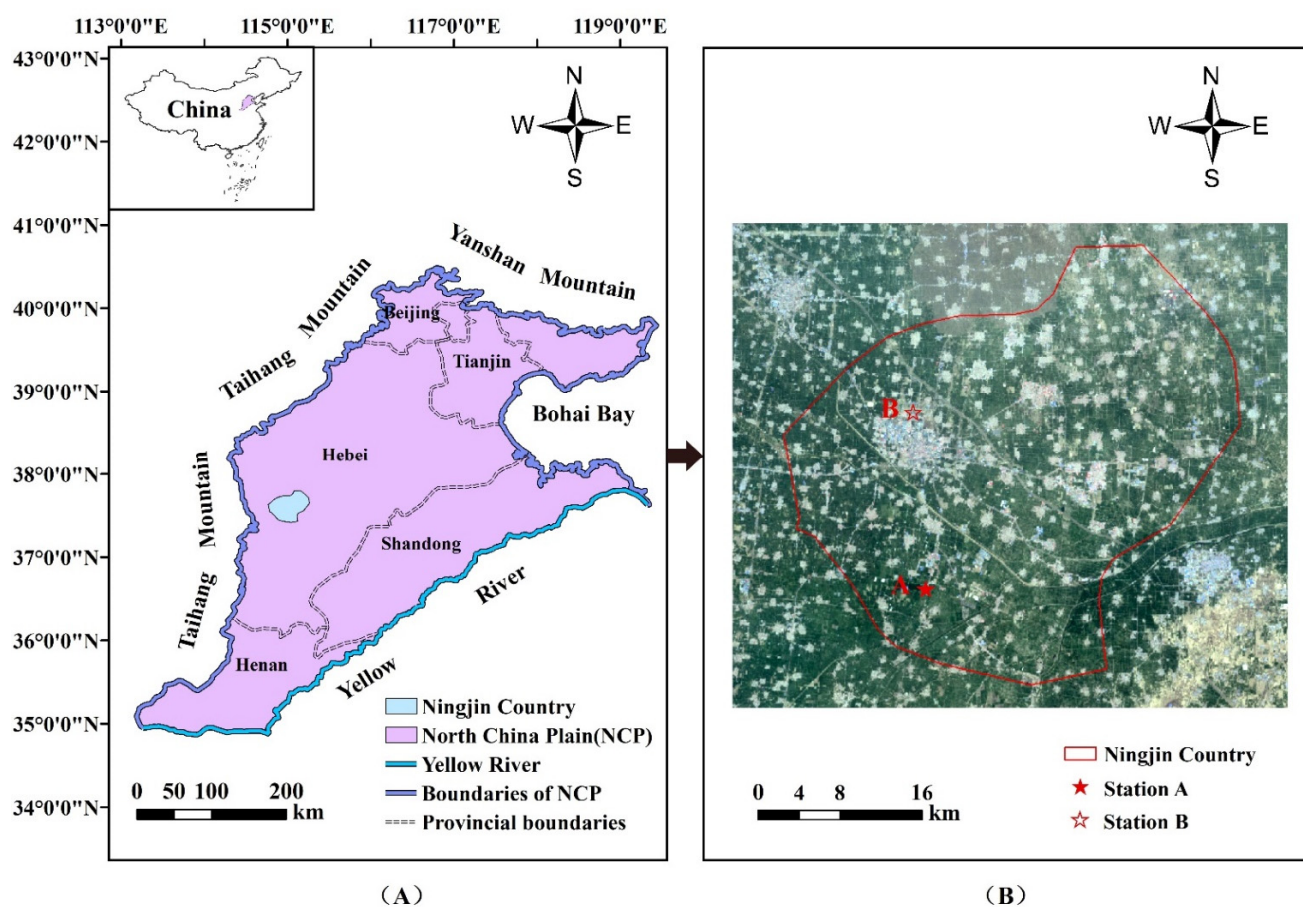


Figure 1. The locations of the experimental site at Station A and National Meteorological Station B in the North China Plain. (A) The location of Ningjin Country in North China Plain. (B) The locations of Stations A and B in Ningjin Country.

Table 1. Sprinkler irrigation schedule after overwintering in the four winter wheat seasons.

Seasons	March		April					May							
	27	29	1	15	16	19	23	4	5	8	12	19	23	25	27
2017–2018	-	-	42	-	35	-	-	-	21 *	-	-	-	-	-	28 *
2018–2019	-	36	-	-	-	-	35	-	-	37 *	-	25 *	-	25 *	-
2019–2020	40 *	-	-	31 *	-	-	-	50	-	-	12	-	-	-	-
2020–2021	-	-	-	-	-	50	-	-	-	50 *	-	-	15	-	-

Note: “*” indicates no or little rainfall (<5 mm) within 3 days after irrigation.

2.3. Data Collection

Microclimate data in the four wheat seasons (from 2017 to 2021) in the sprinkler-irrigated field at Station A were measured using a microclimate station. This microclimate station was installed at the center of the experimental field and consisted of a datalogger (CR1000, Campbell Scientific Inc., Logan, UT, USA), temperature and humidity sensors (PTS-3), a wind sensor (EC-9S), and total and net radiation sensors (TBQ-2, TBB-1, Jinzhou Sunshine Meteorological Technology Co., Ltd., Jinzhou, China). All climatic sensors were installed at a height of 2 m. These microclimate data were sampled for 10 s, and a 30 min average was recorded. A 20-cm-diameter pan was installed on the top of wheat canopy near the microclimate station A to measure water evaporation (E_{pan}), which was used to calculate the irrigation amount [32].

To investigate the water and heat flux during and after sprinkler irrigation, an eddy covariance system (EC system) was installed at the center of the experimental field in

the 2019–2020 and 2020–2021 winter wheat growth seasons. The EC system consisted of an open-path H₂O analyzer (LI-7500DS, LI-COR Inc., Lincoln, NE, USA) to measure the atmospheric H₂O and heat fluxes, a three-dimensional sonic anemometer (WindMaster Pro3-Axis Anemometer, Gill Instruments, Hampshire, UK) to measure the orthogonal components of wind speed fluctuations, and two heat flux plates (HFP01, Hukseflux, Delft, The Netherlands) to measure the soil heat fluxes. Except for the heat flux plates, which were installed at a soil depth of 0.05 m, all sensors were mounted at a height of 1.5 m to ensure complete exposure in all directions (the maximum height of the wheat canopy was approximately 0.8 m above the ground). The raw turbulence EC data were recorded at 10 Hz and stored on a removable 16G flash disk. The SmartFlux System and EddyPro Software (Li-COR Inc., Lincoln, NE, USA) were automatically operated on a powerful microcomputer to compute the final H₂O and heat flux results at 30 min intervals, as the data were logged. The data were automatically postprocessed with despiking, time delay removal, coordinate rotation, sonic temperature correction, frequency correction, and Webb–Pearman–Leuning (WPL) density correction.

Before overwintering, three plots in the experimental field were selected as continuous observation sites. Each plot had three 1 m rows with well-growing wheat plants. After overwintering, the wheat stem number of each 1 m length row was counted to estimate the growth density every two weeks. Additionally, 20 wheat plants near the sample plots were collected for leaf area measurement. The leaf area index (LAI) was calculated as $LAI = (LA_{\text{mean}} \times N_{\text{plant}}) / (L \times W)$, where LA_{mean} is the mean leaf area per plant (m²), N_{plant} is the mean plant number per 1 m length, and L and W are the length and width of the sample plot, which were 1 and 0.15 m, respectively.

The temperature, humidity, and solar radiation sensors at the national meteorological station are generally 1.5 m above the ground, while the wind sensor is 10 m above the ground [30]. The hourly meteorological data can be downloaded from the China Meteorological Data Sharing Service System (<http://cdc.nmic.cn/home.do>) (accessed on 30 July 2021).

2.4. Calculation of Energy Balance and Crop Evapotranspiration ET

The surface energy balance equation can be described as follows [33]:

$$R_n = LE + H + G \quad (1)$$

where R_n is net radiation; LE is the latent flux; H is the sensible heat flux; and G is the soil heat flux at the soil surface. All units are $W m^{-2}$ ($1 W m^{-2} = 1 J m^{-2} s^{-1} = 0.00864 MJ m^{-2} d^{-1}$).

R_n was calculated by the following formula:

$$R_n = R_{si} - R_{so} + R_{li} - R_{lo} \quad (2)$$

where R_{si} and R_{li} are the shortwave and longwave radiation incoming from the atmosphere into the wheat field systems, respectively. R_{so} and R_{lo} are the shortwave and longwave radiation reflected from wheat field systems into the atmosphere, respectively. All units are $W m^{-2}$. The wave band of R_{si} and R_{so} in the total radiation sensor was from 280 to 3000 nm, while that of R_{li} and R_{lo} in the net radiation sensor was from 280 to 50,000 nm.

The surface reflectance rate (SR) represents the ability of the ground to absorb and reflect solar radiation [34]. In this study, SR during the daytime (9:00–16:00) was calculated based on the following formulas:

$$SR = \frac{R_{so}}{R_{si}} \quad (3)$$

The EC system can accurately capture evapotranspiration information of crops in a field [19,35]. The evapotranspiration of winter wheat under sprinkler irrigation at Station A (ET_a) was calculated as follows [36]:

$$ET_a = \frac{LE}{\lambda \rho_w} \quad (4)$$

where ET_a was the measured crop evapotranspiration in the winter wheat field (mm d^{-1}); LE is the latent heat flux ($\text{MJ m}^{-2} \text{d}^{-1}$); λ is the latent heat of vaporization of water (2.45 kJ g^{-1}); ρ_w is water density (1 g cm^{-3}).

The daily reference crop evapotranspiration (ET_0) was calculated by the Penman–Monteith formula recommended by the FAO [37]:

$$ET_0 = \frac{0.408\Delta(R_n - G) + \gamma \frac{900}{T_{\text{mean}} + 273} u_2 \text{VPD}}{\Delta + \gamma(1 + 0.34u_2)} \quad (5)$$

$$\text{VPD} = e_s - e_a \quad (6)$$

$$e_s = \frac{1}{2} \left[0.6108 \exp\left(\frac{17.27T_{\text{max}}}{T_{\text{max}} + 237.3}\right) + 0.6108 \exp\left(\frac{17.27T_{\text{min}}}{T_{\text{min}} + 237.3}\right) \right] \quad (7)$$

$$e_a = e_s \frac{\text{RH}}{100} \quad (8)$$

where ET_0 is the daily reference crop evapotranspiration (mm d^{-1}); R_n is the net radiation ($\text{MJ m}^{-2} \text{d}^{-1}$); G is the soil heat flux ($\text{MJ m}^{-2} \text{d}^{-1}$); T_{mean} , T_{max} , and T_{min} are the mean, maximum, and minimum temperature, respectively ($^{\circ}\text{C}$); Δ is the slope of the vapor pressure curve ($\text{kPa } ^{\circ}\text{C}^{-1}$); γ is the psychrometric constant ($\text{kPa } ^{\circ}\text{C}^{-1}$); VPD is vapor pressure deficit (kPa); e_s is the saturated vapor pressure at air temperature (kPa); e_a is the actual vapor pressure (kPa); u_2 is the wind speed at a height of 2 m (m s^{-1}); and RH is daily relative humidity (%). In particular, the wind speed measured by the national station was at a height of 10 m (u_{10} , m s^{-1}), which was converted into that at a height of 2 m by the following formula [37]:

$$u_2 = u_{10} \frac{4.87}{\ln(67.8 \times 10 - 5.42)} \quad (9)$$

The difference in daily ET_0 (ΔET_0 , mm d^{-1}) under sprinkler irrigation and non-irrigation conditions was calculated as follows:

$$\Delta ET_0 = ET_{0,n} - ET_{0,s} \quad (10)$$

where $ET_{0,n}$ is daily ET_0 under non-irrigation conditions, which was calculated using the adjusted data at national meteorological station by considering the system bias (mm d^{-1}), and $ET_{0,s}$ is daily ET_0 under sprinkler irrigation conditions (mm d^{-1}).

The crop coefficient K_c in the field was calculated as follows:

$$K_c = \frac{ET_a}{ET_{0,s}} \quad (11)$$

The crop evapotranspiration without considering the effect of sprinkler irrigation on field microclimate was estimated as follows:

$$ET_c = ET_{0,n} \cdot K_{c,n} \quad (12)$$

where $K_{c,n}$ is K_c not affected by sprinkler irrigation, and was calculated by the mean value of K_c in the 4–5 days before each sprinkler irrigation.

Then, the variation in crop evapotranspiration caused by sprinkler irrigation (ΔET , mm d^{-1}) was calculated by ET_a minus ET_c as follows:

$$\Delta ET = ET_a - ET_c \quad (13)$$

2.5. Data Analysis

Since most sprinkler irrigations were performed during the period from jointing to milking of winter wheat, the irrigation events during this period were analyzed. There were a total of 16 irrigation events in the four wheat seasons (Table 1), eight of which were affected by precipitation and excluded from the data analysis. Finally, another eight sprinkler irrigation events, labeled from I1 to I8, were chosen for data analysis (Table 1). Detailed information on the eight selected sprinkler irrigation events is described in Table 2.

Table 2. Irrigation date, irrigation amount, wheat growth stage and leaf area index (LAI) in irrigation events I1–I8. Data in I1–I6 were used for microclimate change model development and those in I7 and I8 were used for model validation.

Irrigation Events	Model Development						Model Validation	
	I1	I2	I3	I4	I5	I6	I7	I8
Date	27 March 2020	5 May 2018	8 May 2019	19 May 2019	25 May 2019	8 May 2021	27 May 2018	15 April 2020
Amount (mm)	40	21	37	25	25	50	28	31
Growth stages	Earlier period of jointing	Earlier period of milking	Earlier period of milking	Middle period of milking	Later period of milking	Earlier period of milking	Later period of milking	Later period of jointing
LAI	3.7	5.3	5.2	4.8	2.0	4.0	1.3	7.0

Due to the different sites and underlying situations, there were some differences in the meteorological data between the field and the national station, which can be regarded as the system bias. Since crop coverage could affect these system biases, the mean system bias of five days not affected by rainfall before each sprinkler irrigation was used to adjust the meteorological data at the national station. During sprinkler irrigation and in the 10 days after sprinkler irrigations, the meteorological data in the national station were rebuilt by considering the corresponding system biases, which was treated as the data under non-irrigation conditions. Then, the differences in meteorological data in the sprinkler-irrigated field and the rebuilt ones under non-irrigation conditions were considered as the effect of sprinkler irrigation.

To explore the energy balance under sprinkler irrigation in the wheat field, the changes in field energy indices, including surface reflectance (SR), the rate of latent heat to net radiation (LE/R_n), the rate of sensible heat to net radiation (H/R_n), and soil heat flux to net radiation (G/R_n), before and after sprinkler irrigation at Station A in typical events I1 (in the earlier period of jointing, LAI was 3.7 and irrigation amount was 40 mm) and I6 (in the earlier period of milking, LAI was 4.0 and irrigation amount was 50 mm) were analyzed. Then, ET_0 and ET_c under sprinkler irrigation were compared to those under non-irrigation conditions to analyze the impact of sprinkler irrigation on crop ET. Moreover, we further explored the relationship between the increasing ET and the change in microclimate. Data were analyzed by SPSS 21 (SPSS, Inc., Chicago, IL, USA) with the linear regression method, when p value of one-way analysis of variance (ANOVA) was less than 0.05, indicating there was a significant relationship between the increasing ET and the change in microclimate.

2.6. Microclimate Change Model Development and Validation

To quantify the changes in temperature, RH, and VPD after sprinkler irrigation, data on sprinkler irrigation events from I1 to I6 were used to develop microclimate models. Sprinkler irrigation events from I1 to I6 were implemented under different growth stages and irrigation water amounts. Event I1 was in the earliest growth stage of wheat with the smallest LAI; I2 and I3 had similar LAIs, but different irrigation amounts; I4 and I5 had similar irrigation amounts, but different LAIs; and I6 had the largest irrigation

amount. Data for events I7 and I8 (moderate irrigation amount) were used to verify models. During the microclimate models development process, the considered factors included the irrigation factor (the irrigation amount), time factor (days after irrigation), crop factor (the LAI of wheat), weather status (sunny, cloud, overcast, and rain), and microclimate condition (the mean temperature T_{mean} , net radiation R_n , relative humidity RH, and wind speed u) at Station B. The independent variables of the model are shown in Table 3.

Table 3. Independent variables used in microclimate change development.

Independent Variable	Irrigation Factor	Time Factor	Crop Factor	Weather Factor				Meteorological Factors			
	X_1	X_2	X_3	X_4	X_5	X_6	X_7	X_8	X_9	X_{10}	X_{11}
Name	Irrigation Amount	Days after irrigation	LAI	Sunny	Cloud	Overcast	Rain	T_{mean}	R_n	RH	u
Unit	mm	day	-	-	-	-	-	$^{\circ}C$	$MJ\ m^{-2}\ d^{-1}$	%	$m\ s^{-1}$
Station	A	A	A	B	B	B	B	B	B	B	B

Stepwise regression method is a multiple linear regression model, which aims to select and eliminate the variables causing multiple collinearity and establish the optimal relationship model between independent variables and dependent variables [38]. In this study, the stepwise regression method was used in Stata/SE 15.1 software (StataCorp, College Station, TX, USA) to select variables from all the considered indices and establish the optimal model. The weather factor was defined using the classical approach of “dummy variables” [39]. The actual weather type in a day was set to 1, and the other weather types were set to 0. For example, on cloudy days, the value of cloud variables was 1, and the values of sunny, overcast, and rain variables were set to 0. During the process of variable screening, the significance level of the introduced variables and eliminated ones were set as $p < 0.18$ and $p > 0.25$ to obtain the optimal independent variables, respectively. Then, new variables were introduced one by one, while the old ones were screened one by one, until no new variables were introduced, and no old ones were eliminated. Finally, the regression models between the selected independent variables and dependent variables were established.

The microclimate change models were evaluated by the indices of the coefficient of determination (R^2), root mean square error (RMSE), mean relative error (MRE) and consistency index (d) [40]. The four indices were calculated as follows:

$$R^2 = \left[\frac{\sum_{i=1}^n (O_i - O)(S_i - S)}{\sqrt{\sum_{i=1}^n (O_i - O)^2} \sqrt{\sum_{i=1}^n (S_i - S)^2}} \right]^2 \tag{14}$$

$$RMSE = \sqrt{\frac{1}{n} \sum_{i=1}^n (S_i - O_i)^2} \tag{15}$$

$$MRE = \frac{1}{n} \sum_{i=1}^n \frac{S_i - O_i}{O_i} \times 100\% \tag{16}$$

$$d = 1 - \frac{\sum_{i=1}^n (S_i - O_i)^2}{\sum_{i=1}^n (|S_i - O| + |O_i - O|)^2} \tag{17}$$

where S_i is the i th simulated value, S is the mean of the simulated values; O_i is the i th observed value, O is the mean of the observed values, and n is the number of paired observed simulated values.

The evaluation criteria were as follows: values of R^2 , RMSE, MRE and d are between 0 and 1, and values of R^2 and d closer to 1 and those of RMSE and MRE closer to 0 reveal better model performance [40,41]. During the model development and validation stage, the values of R^2 and d between the observed and simulated microclimate changes were between 0.71 and 0.87 and 0.90 and 0.95, respectively. The RMSE values were within 0.25 $^{\circ}C$ for both ΔT_{min} and ΔT_{max} , 1.70% for ΔRH , and 0.05 kPa for ΔVPD . The MREs of

the ΔT_{\min} , ΔT_{\max} , ΔRH , and ΔVPD were between -20% and 17% (Figure 2). These indices implied that the developed models could perform well in predicting ΔT_{\min} , ΔT_{\max} , ΔRH , and ΔVPD after sprinkler irrigation.

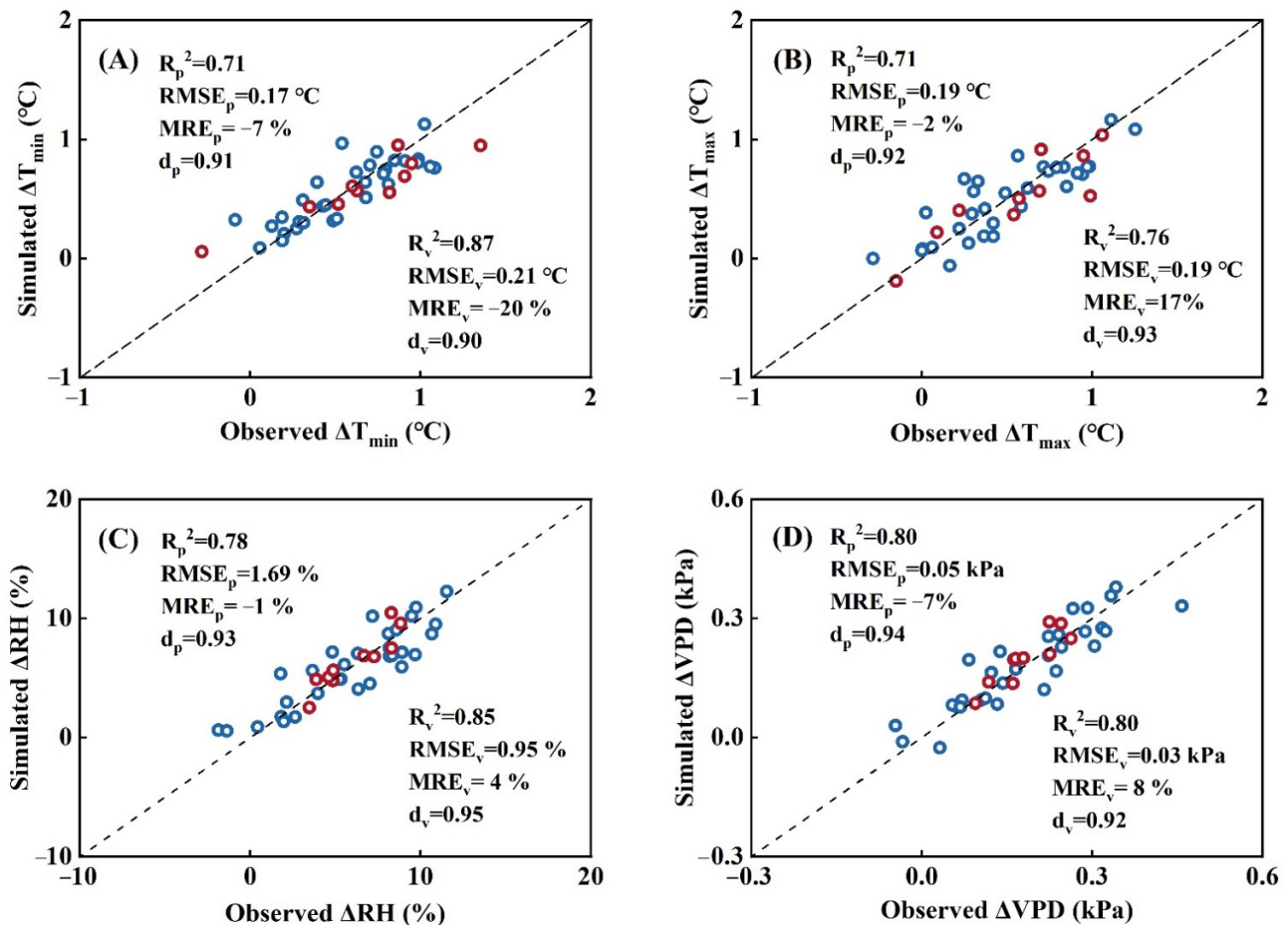


Figure 2. Simulated and observed values for the changes in daily T_{\min} (A) and T_{\max} (B), daily mean RH (C) and VPD (D) under sprinkler irrigation conditions compared to those under non-irrigation conditions after sprinkler irrigation in events I1–I8. The subscripts “p” and “v” represent the evaluation indications during the model development and validation stages, respectively.

3. Results

3.1. System Biases

With no sprinkler irrigation, the daily minimum (T_{\min}) was approximately 2.0 °C higher, daily maximum temperatures (T_{\max}) was 0.4 °C higher, and relative humidity (RH) was 6.4% lower in the sprinkler-irrigated field than at the national station (Figure 3A–C). After the data at Station B were rebuilt in consideration of the corresponding system biases presented in Table 4, the R^2 between the data in the sprinkler-irrigated field and the adjusted data at the national meteorological station were all 0.99 for the T_{\min} , T_{\max} and RH, and the corresponding RMSE 0.3 °C , 0.2 °C , and 1% , respectively (Figure 3D,E). These results indicate that the adjusted data at Station B can be regarded as corresponding to the data at Station A under non-irrigation conditions.

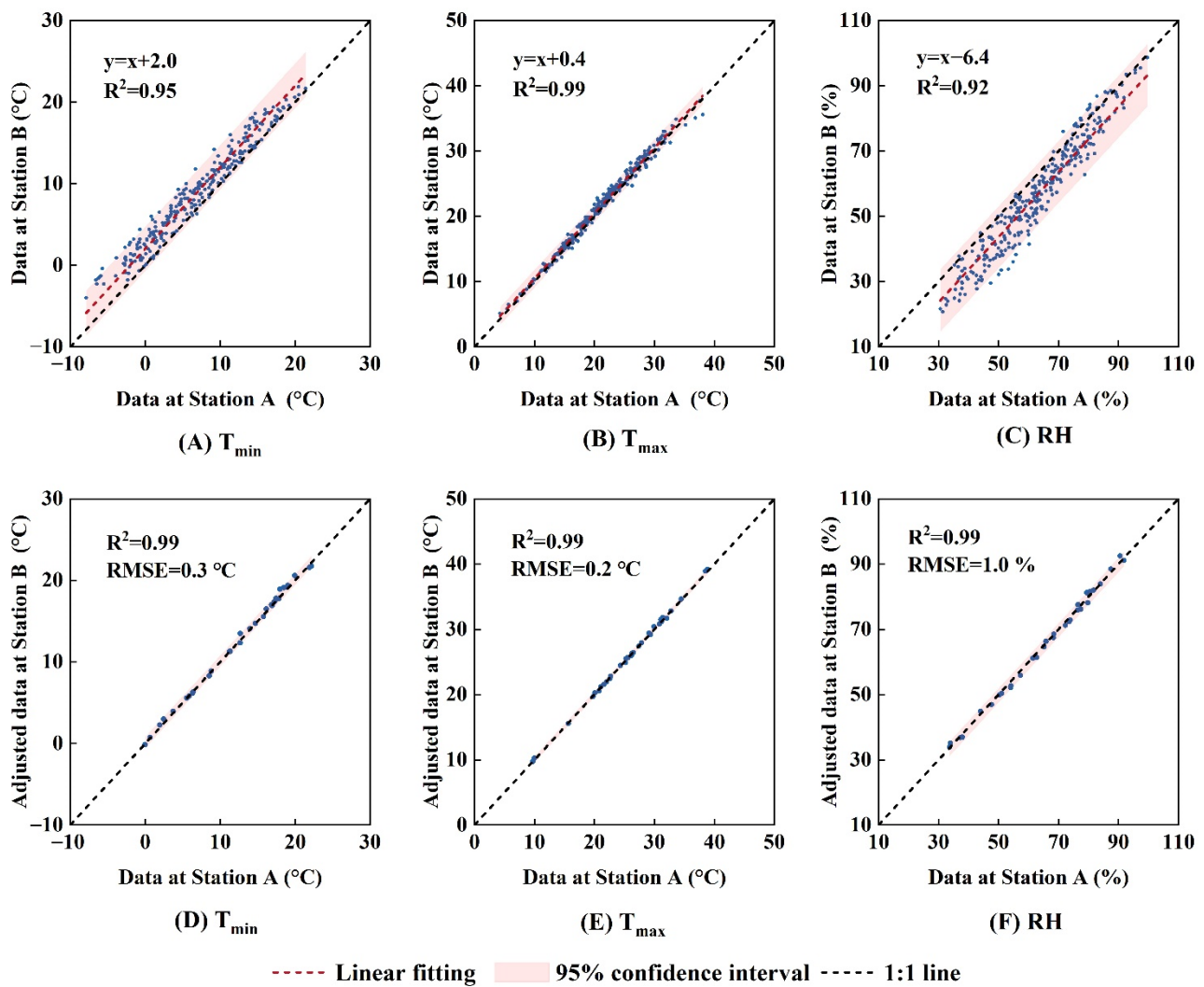


Figure 3. Comparison of microclimatic variables in the sprinkler-irrigated field and the measured and adjusted data by considering the system bias at the national meteorological station. (A–C) Daily maximum temperature (T_{\max}), minimum temperature (T_{\min}), and relative humidity (RH) in the sprinkler-irrigated field and those at the national meteorological station from March to May in the 2017–2021 wheat season, when there were no sprinkler irrigations. (D–F) T_{\max} , T_{\min} , and RH in the sprinkler-irrigated field and the correspondingly adjusted T_{\max} , T_{\min} , and RH at the national meteorological station in the five days before sprinkler irrigations.

Table 4. The mean systematic bias of daily minimum (T_{\min}) and maximum temperatures (T_{\max}), and relative humidity (RH) between the sprinkler-irrigated field and the national meteorological station in the five days before each irrigation event.

Irrigation Events	I1	I2	I3	I4	I5	I6	I7	I8
T_{\min} ($^{\circ}\text{C}$)	0.39	1.46	2.01	1.89	1.89	2.57	2.71	1.66
T_{\max} ($^{\circ}\text{C}$)	0.24	0.47	0.61	0.61	0.61	0.48	0.87	0.24
RH (%)	5.23	7.62	5.53	6.35	6.35	4.96	7.53	5.31

3.2. Microclimate Changes

3.2.1. Daily Minimum Temperature (T_{\min})

The daily T_{\min} under sprinkler irrigation conditions was lower than that under non-irrigation conditions after sprinkler irrigation, and this dropping or cooling effect lasted for 3–6 days (Figure 4). The maximum ΔT_{\min} reached 1.4 $^{\circ}\text{C}$ on the third day after sprinkler

irrigation. Generally, ΔT_{\min} varied slightly, with a mean value of approximately $0.8\text{ }^{\circ}\text{C}$ in the first three days after irrigation, after which it decreased gradually with time (Figure 4F).

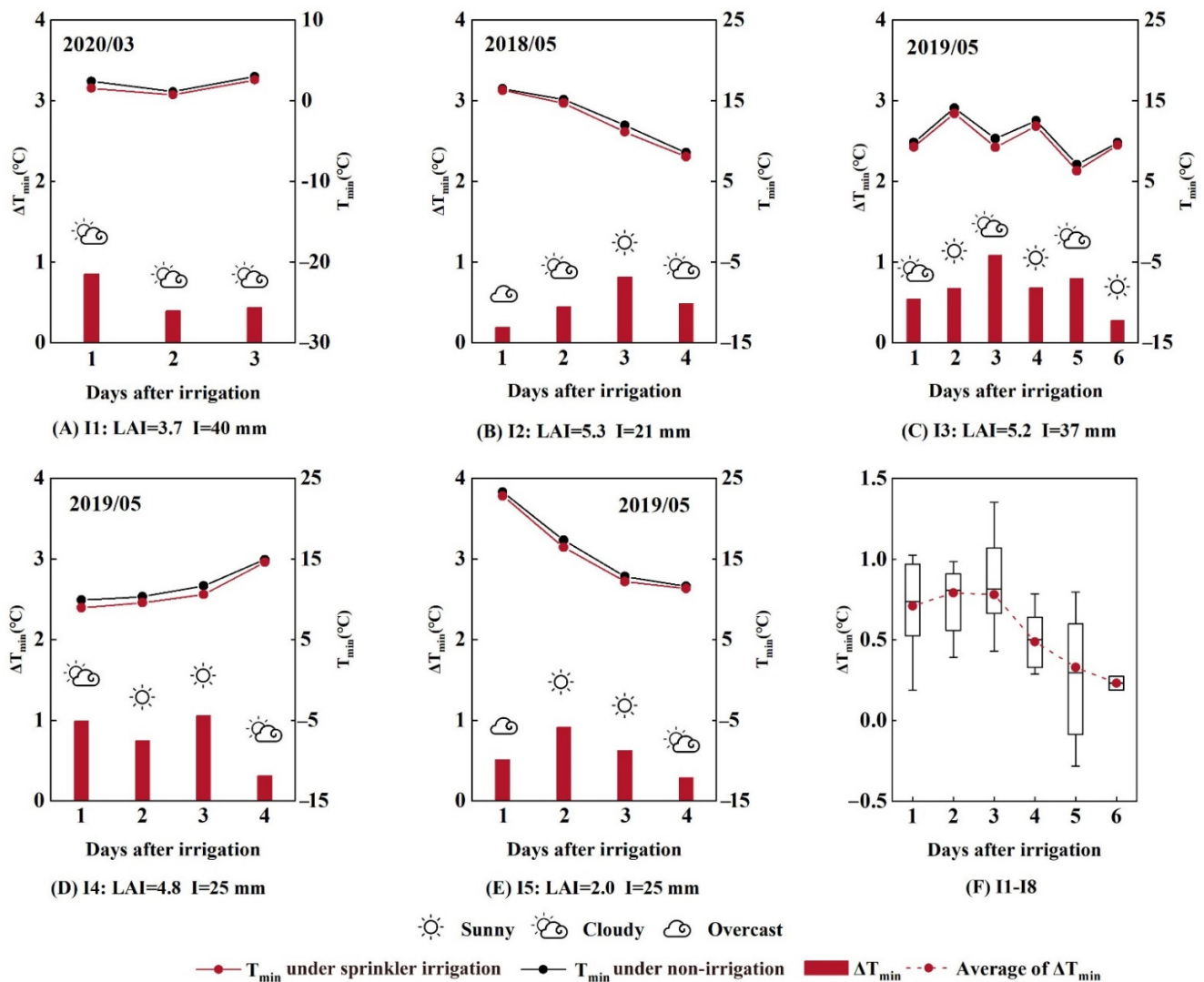


Figure 4. Daily minimum temperature (T_{\min}) and its difference (ΔT_{\min}) between sprinkler irrigation and non-irrigation conditions in the days after sprinkler irrigation. (A–E) Changes of T_{\min} and ΔT_{\min} in irrigation events I1–I5. (F) Box-plot of ΔT_{\min} in events I1–I8. ΔT_{\min} was calculated as T_{\min} under non-irrigation conditions minus that under sprinkler irrigation conditions. A positive T_{\min} indicates a cooling effect in the sprinkler-irrigated field.

The cooling effect of sprinkler irrigation, indicated by a positive ΔT_{\min} , varied with plant growth, irrigation depth, and microclimate status. At the early jointing stage, with short plants, small LAI, and lower temperature for event I1, the cooling effect with positive ΔT_{\min} lasted for 3 days after sprinkler irrigation (Figure 4A), and the maximum ΔT_{\min} was $0.9\text{ }^{\circ}\text{C}$ and occurred on the first day after irrigation. The cooling effect of the sprinkler on daily T_{\min} lasted for 4 and 6 days, with corresponding irrigation depths of 21 and 37 mm in events I2 and I3, respectively, when both sprinkler events were carried out in the earlier period of milking stage (Figure 4B,C). The maximum daily ΔT_{\min} was $0.8\text{ }^{\circ}\text{C}$ in I2 and $1.1\text{ }^{\circ}\text{C}$ in I3, and both occurred on the third day after irrigation. This indicated that a greater irrigation depth could induce longer and stronger cooling effects on daily T_{\min} . In the middle and later period of milking (Figure 4D,E), for events I4 and I5 with the same irrigation depth, a larger LAI of 4.8 for event I4 resulted in a higher ΔT_{\min} ($1.1\text{ }^{\circ}\text{C}$) compared to that ($0.9\text{ }^{\circ}\text{C}$) for event I5 with an LAI of 2, but the cooling duration in both

events was 4 days. On overcast days, the ΔT_{\min} was generally lower, indicating that the weather status also affected the sprinkler cooling effect (Figure 4B,E).

3.2.2. Daily Maximum Temperature (T_{\max})

The daily T_{\max} under sprinkler irrigation conditions decreased after sprinkler irrigation, and this cooling effect lasted for 3–5 days after irrigation (Figure 5). From sprinkler irrigation I1 to I5, the maximum ΔT_{\max} s were 0.6, 0.9, 1.3, 1.0, and 0.9 °C, respectively (Figure 5A–E), all of which occurred in the first three days after irrigation. In general, the ΔT_{\max} decreased from approximately 0.9 °C on the first day after sprinkler irrigation to near zero on the sixth day (Figure 5F).

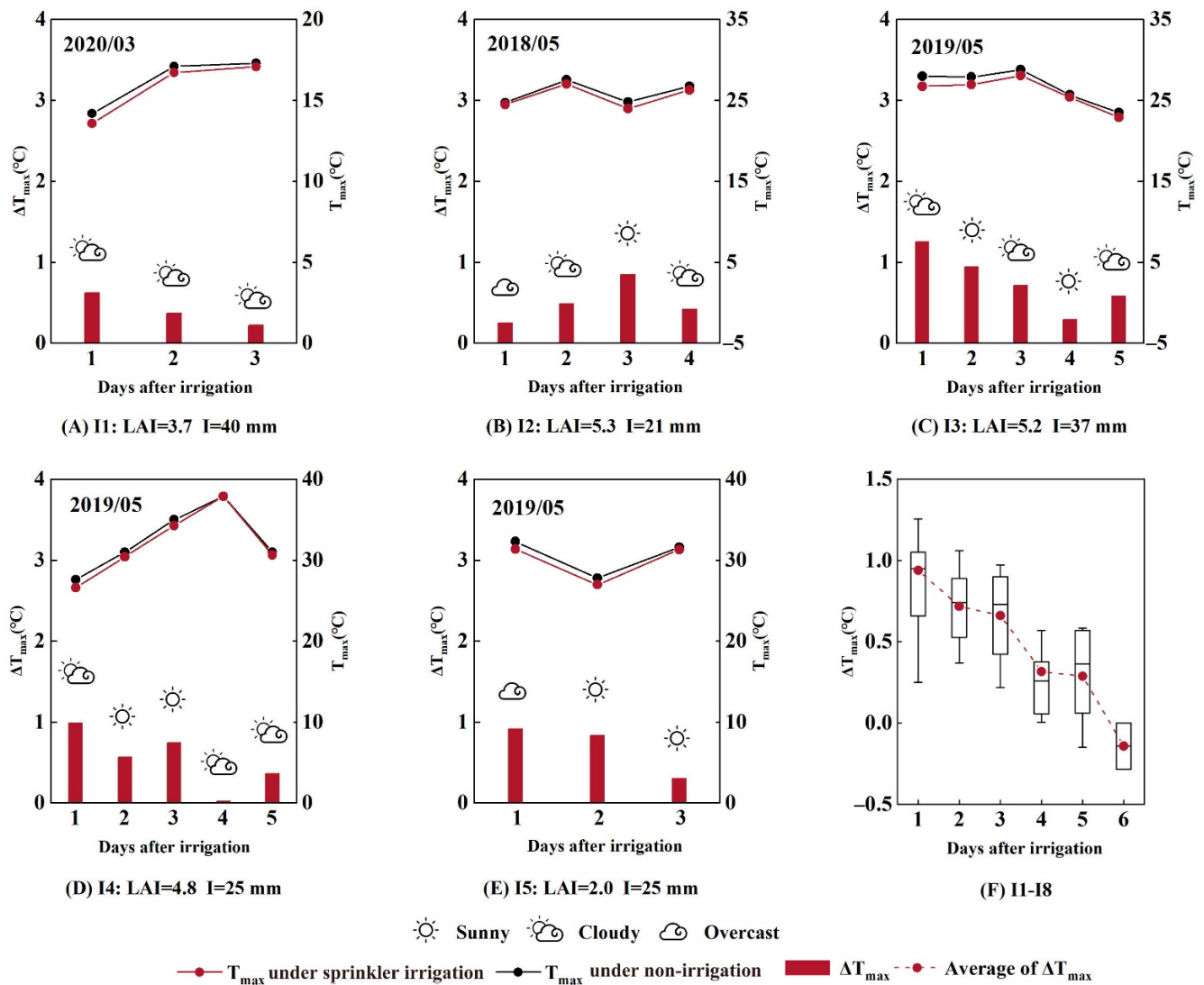


Figure 5. Daily maximum temperature (T_{\max}) and its difference (ΔT_{\max}) between sprinkler irrigation and non-irrigation conditions in the days after sprinkler irrigation. (A–E) Changes of T_{\max} and ΔT_{\max} in irrigation events I1–I5. (F) Box-plot of ΔT_{\max} in events I1–I8. ΔT_{\max} was calculated as T_{\max} under non-irrigation irrigation minus that under sprinkler irrigation. A positive ΔT_{\max} indicates a cooling effect in the sprinkler-irrigated field.

3.2.3. Daily Mean Relative Humidity (RH)

The daily mean RH under sprinkler irrigation conditions was higher than that under non-irrigation conditions after sprinkler irrigation (Figure 6), and this condition lasted for approximately 3, 4, 7, 5, and 4 days for sprinkler events from I1 to I5 (excluding an overcast day on the first day after irrigation in sprinkler I5), respectively. The maximum ΔRH s were

8.1, 8.2, 10.7, 10.9, and 8.9%, respectively, from I1 to I5. Considering all eight irrigation events, the ΔRH s in the first three days after irrigation were close, and approximately 7.5%, after which they decreased to 2.0% on the 6th to 7th days (Figure 6F).

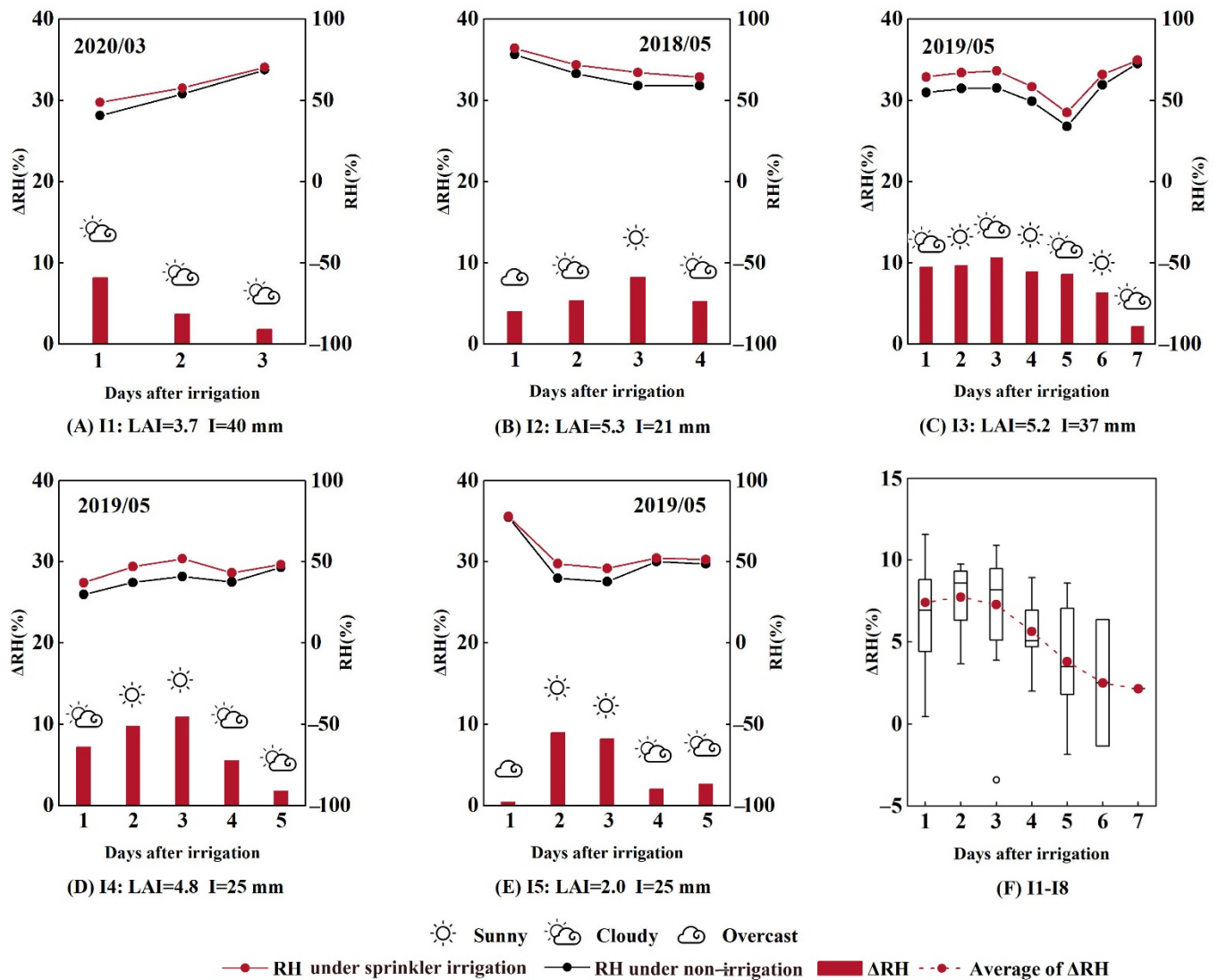


Figure 6. Daily relative humidity (RH) and its difference (ΔRH) between sprinkler irrigation and non-irrigation conditions in the days after sprinkler irrigation. (A–E) Changes of RH and ΔRH in irrigation events I1–I5. (F) Box-plot of ΔRH in events I1–I8. ΔRH was calculated as RH under sprinkler irrigation conditions minus that under non-irrigation conditions. A positive ΔRH means an increased RH in the sprinkler-irrigated field.

3.2.4. Daily Mean Vapor Pressure Deficit (VPD)

Compared with non-irrigation, the daily mean VPD under sprinkler irrigation was lower after sprinkler irrigation, and this situation lasted for 3–7 days after irrigation (Figure 7). The maximum ΔVPD s ranged from 0.12 to 0.46 kPa, with a mean value of 0.39 kPa. When all ΔVPD data in irrigation events I1–I8 were pooled together, the mean ΔVPD s in the first three days after sprinkler irrigation were higher, at approximately 0.25 kPa, and then they decreased to lower than 0.05 kPa on the 6th and 7th days. It should be noted that the ΔVPD on overcast days was lower than 0.10 kPa (Figure 7B,E).

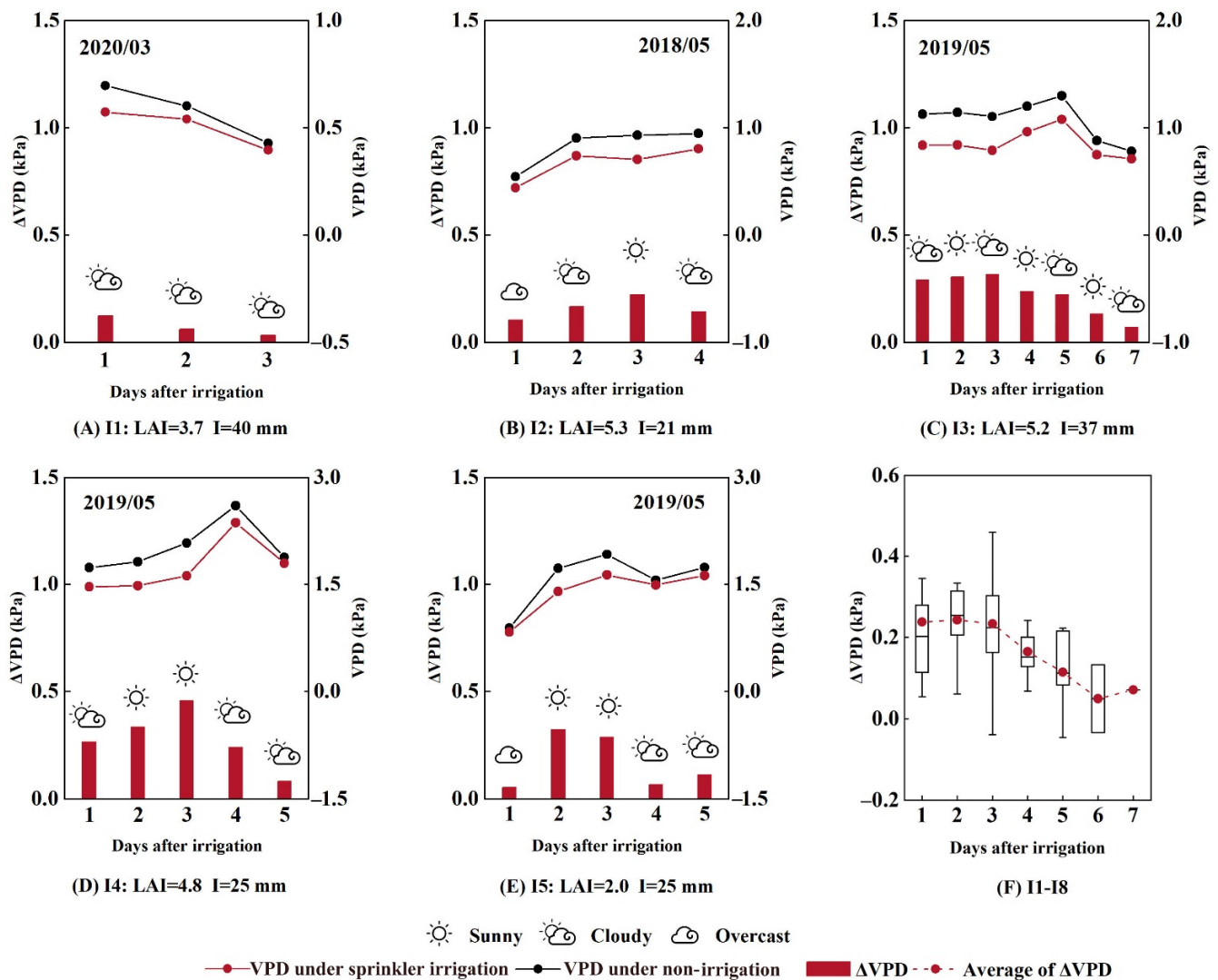


Figure 7. Daily vapor pressure deficit (VPD) and its difference (Δ VPD) between sprinkler irrigation and non-irrigation conditions in the days after sprinkler irrigation. (A–E) Changes of VPD and Δ VPD in irrigation events I1–I5. (F) Box-plot of Δ VPD in events I1–I8. Δ VPD was calculated as VPD under non-irrigation conditions minus that under sprinkler irrigation conditions. A positive VPD means a decreased VPD in the sprinkler-irrigated field.

3.3. Change of Field Energy Balance

The daily R_n varied slightly during the 4 days before irrigation, and the daily SR also varied slightly, with mean values of 0.19 for event I1 and 0.18 for event I6 (Figure 8A,B). After sprinkler irrigation, the mean values of SR in the following 3 days decreased by 0.01 for both events, although R_n was close to that before sprinkler irrigation (Figure 8A,B). This decrease in SR indicated that there was more available solar energy in the crop-soil system after irrigation. The mean value of LE/R_n in the 3 days after irrigation was 0.19 and 0.23 higher for events I1 and I6, respectively, than that before sprinkler irrigation (Figure 8C,D). The increased rate of LE/R_n finally resulted in the daily water flux increasing by approximately 27% in the 1–3 days after sprinkler irrigation. The H/R_n showed a downwards trend in both events after irrigation. The mean values of H/R_n before irrigation were 0.14 and 0.02 for events I1 and I6, respectively, and dropped to 0.08 and -0.15 in the following 3 days after sprinkler irrigation (Figure 8E,F). This indicated that the sensible heat percentage decreased after irrigation. The daily G/R_n after sprinkler irrigation changed

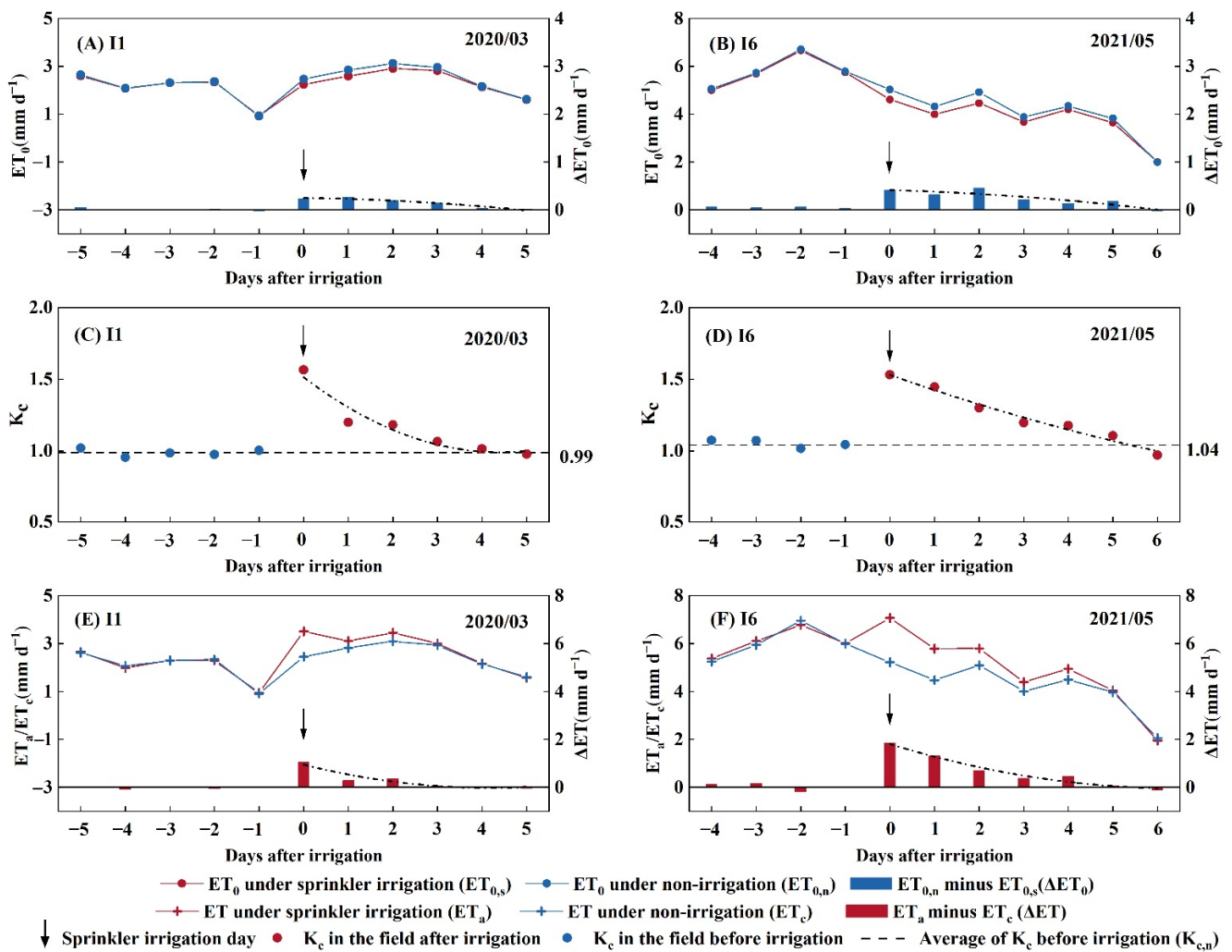


Figure 9. Changes in reference crop evapotranspiration (ET_0) and its difference (ΔET_0) between sprinkler irrigation and non-irrigation conditions, crop coefficient (K_c) in the field, and crop evapotranspiration (ET) and its difference (ΔET) between sprinkler irrigation and non-irrigation conditions in irrigation events I1 (A,C,E) and I6 (B,D,F).

The crop coefficient K_c in the field showed an obvious upwards trend after irrigation (Figure 9C,D). On the day of sprinkler irrigation, values of K_c were 1.56 and 1.53 for irrigation events I1 and I6, which were much higher than that before irrigation (0.99 and 1.04 in events I1 and I6, respectively). After irrigation, K_c dropped gradually and reached 0.99 on the fourth day in event I1 and 1.04 on the fifth day in event I6. The dramatic rise in K_c after sprinkler irrigation implies a large increase in ET_a . Compared with ET_c under non-irrigation (Figure 9E,F), higher ET_a was found at days 3 and 5 under I1 and I6 sprinkler irrigation. This finally resulted in crop ET 1.8 and 4.7 mm higher for the I1 and I6 sprinkler irrigations, respectively, compared to that under non-irrigation conditions.

3.5. Relationship between Increasing ET and the Change in Microclimate

Figure 10 clearly shows that ΔT_{min} , ΔT_{max} , ΔRH , and ΔVPD increased with increasing ΔET , and the positive relationships between ΔET and ΔT_{min} , ΔT_{max} , ΔRH , and ΔVPD were significant at the level of 0.05. This indicates a strong mutual feedback relationship between the increasing ET and the microclimate change in the sprinkler-irrigated field.

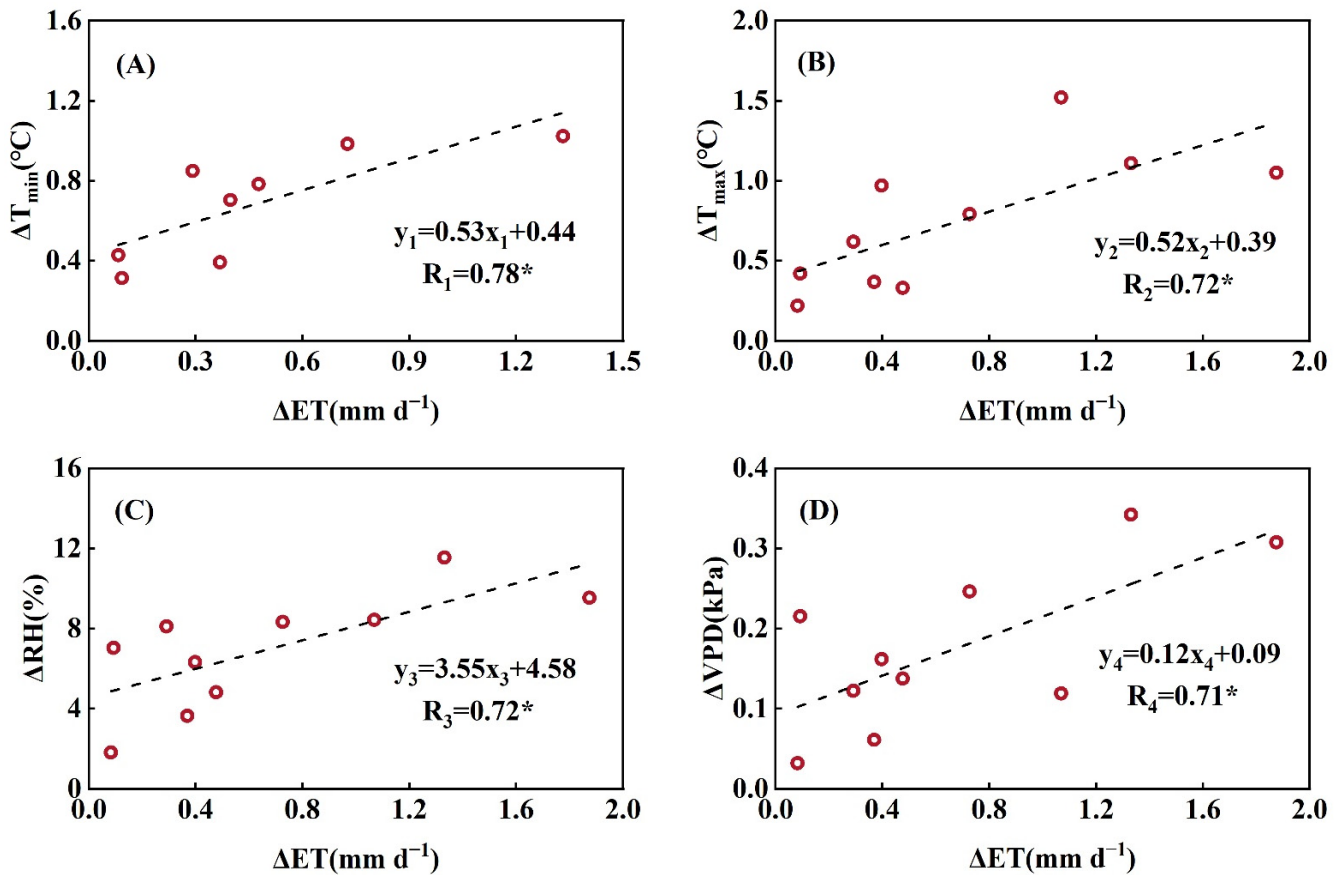


Figure 10. The relationship of increased crop evapotranspiration (ΔET) and changes in daily minimum temperature (ΔT_{\min}) (A) and maximum temperature (ΔT_{\max}) (B), and daily mean relative humidity (ΔRH) (C) and vapor pressure deficit (ΔVPD) (D) under sprinkler irrigation and non-irrigation conditions in events I1 and I6. The symbol “*” after the R value means that the regression line is significant at the 0.05 level.

3.6. Quantitative Model of Microclimate Change

The ΔT_{\min} , ΔT_{\max} , ΔRH , and ΔVPD in the days after sprinkler irrigation were fitted by the stepwise regression method, and the results on selected variables with coefficients for each model are listed in Table 5. The irrigation amount, LAI, and sunny weather had a positive effect on these four microclimate indices, while days after irrigation and RH had a negative effect. ΔT_{\min} was negatively correlated with the overcast weather index, ΔT_{\max} was positively correlated with the meteorological index of daily mean temperature (T_{mean}), ΔRH was negatively correlated with the meteorological index of u, and ΔVPD was negatively correlated with the overcast index and u and positively correlated with T_{mean} and R_n . To summarize, the models of ΔT_{\min} , ΔT_{\max} , ΔRH , and ΔVPD in winter wheat fields after sprinkler irrigation in the NCP were as follows:

$$\Delta T_{\min} = 0.008X_1 - 0.09X_2 + 0.04X_3 + 0.21X_4 - 0.11X_6 - 0.007X_{10} + 0.75 \quad (18)$$

$$\Delta T_{\max} = 0.009X_1 - 0.16X_2 + 0.09X_3 + 0.24X_4 + 0.02X_8 - 0.003X_{10} + 0.03 \quad (19)$$

$$\Delta RH = 0.07X_1 - 0.71X_2 + 0.82X_3 + 1.78X_4 - 0.16X_{10} - 1.78X_{11} + 13.43 \quad (20)$$

$$\Delta VPD = 0.002X_1 - 0.03X_2 + 0.03X_3 + 0.05X_4 - 0.02X_6 + 0.008X_8 + 0.004X_9 - 0.005X_{10} - 0.04X_{11} + 0.18 \quad (21)$$

where ΔT_{\min} , ΔT_{\max} , ΔRH , and ΔVPD represent the drop of T_{\min} and T_{\max} (°C), the increase in RH (%), and the decrease in VPD (kPa) under sprinkler irrigation compared to under non-irrigation, respectively; X_1 , X_2 , X_3 , X_4 , X_6 , X_8 , X_9 , X_{10} , and X_{11} are irrigation amount

(mm), days after irrigation (d), LAI at Station A, weather of sunny, weather of overcast, T_{mean} ($^{\circ}\text{C}$), R_n ($\text{MJ m}^{-2} \text{d}^{-1}$), RH (%), and u (m s^{-1}) under non-irrigation, respectively.

Table 5. Selected variables and their corresponding coefficients in the regression models of ΔT_{min} , ΔT_{max} , ΔRH and ΔVPD fitted by stepwise regression. The terms ΔT_{min} , ΔT_{max} , ΔRH , and ΔVPD are changes in the daily minimum and maximum temperature, daily mean relative humidity, and vapor pressure deficit under sprinkler irrigation and non-irrigation conditions.

Independent Variable	Name	Coefficient			
		ΔT_{min}	ΔT_{max}	ΔRH	ΔVPD
X_1	Irrigation Amount	0.008	0.009	0.07	0.002
X_2	Days after irrigation	−0.09	−0.16	−0.71	−0.03
X_3	LAI	0.04	0.09	0.82	0.03
X_4	Sunny	0.21	0.24	1.78	0.05
X_5	Cloud	-	-	-	-
X_6	Overcast	−0.11	-	-	−0.02
X_7	Rain	-	-	-	-
X_8	T_{mean}	-	0.02	-	0.008
X_9	R_n	-	-	-	0.004
X_{10}	RH	−0.007	−0.003	−0.16	−0.005
X_{11}	u	-	-	−1.78	−0.04
X_{12}	Constant	0.75	0.03	13.43	0.18

4. Discussion

4.1. Changes in Energy Fluxes in the Sprinkler Irrigated Field

In this study, SR in the field was found to be reduced by 0.01 after the I1 and I6 sprinkler irrigations (Figure 8). Since the solar radiation coming from the atmosphere into the wheat field systems does not change, the crop–soil system obtains a greater amount of net solar radiation energy. Similarly, due to the decrease in SR, R_n above the rice canopy during 12:00–13:00 increases by 28.82 W m^{-2} after mist spraying 1 mm of water [11]. Furthermore, furrow irrigation has a lower SR than drip irrigation, resulting in a 35 W m^{-2} higher R_n [42]. In the energy balance items, the proportion of latent heat to net radiation, LE/R_n , increased by 0.19–0.23 in the 1–3 days after sprinkler irrigation. Correspondingly, the mean H/R_n in the 3 days after irrigation decreased by 0.06 in event I1 and 0.17 in event I6, while G/R_n had a slight change (Figure 8). Similar results have been reported in previous studies on maize, soybean, rice, and cotton [6,11,19]. The increase in LE/R_n after irrigation means field crop ET increased. Compared with the non-irrigation conditions, the increased ET_{aS} was 1.1, 0.3, and 0.4 mm on the irrigation day and on the 1st and 2nd days after irrigation in event I1, and the corresponding values were 1.9, 1.3, and 0.7 mm in event I6, respectively. The decline in H/R_n after irrigation implied a microclimate change in temperature in the winter wheat field. Compared with non-irrigation, the daily T_{max} in the field dropped by 0.6 and $0.4 \text{ }^{\circ}\text{C}$ on the 1st and 2nd days after sprinkler irrigation in event I1, and T_{min} decreased by 0.9 and $0.4 \text{ }^{\circ}\text{C}$. Similarly, on the 1st and 2nd days after the sprinkler in event 6, the daily T_{max} s decreased by 1.1 and $0.8 \text{ }^{\circ}\text{C}$, respectively, and the daily T_{min} s depressions in both days were $1.0 \text{ }^{\circ}\text{C}$.

The change in energy fluxes in the field was closely related to the content of water vapor in the air. The greater the increase in surface humidity by evapotranspiration in the field after irrigation, the greater the corresponding increase in LE and decrease in H [6]. In this study, the average daily increase in RH within three days after irrigation under sprinkler irrigation conditions was 6.7% and 9.8% higher than that under non-irrigation conditions in events I1 and I6, respectively. Correspondingly, daily LE increased by 2.9 and $3.8 \text{ KJ m}^{-2} \text{d}^{-1}$ and H decreased by 0.3 and $2.1 \text{ KJ m}^{-2} \text{d}^{-1}$. We can conclude that a large increase in RH by ET_a after sprinkler irrigation resulted in a large increase in LE and a large decrease in H in the field.

4.2. Changes in Crop ET_a in the Sprinkler-Irrigated Field

In this study, ET_0 was lower in the sprinkler-irrigated field than that under non-irrigation conditions, indicating a low atmosphere evapotranspiration potential after sprinkler irrigation. This finding was confirmed by the reduced air temperature and VPD and increased RH in the sprinkler-irrigated field (Figures 4–7). Similarly, the water evaporation potential measured using a 20 cm Pan above the crop canopy is 3–11% lower in sprinkler-irrigated fields than in surface irrigation fields [16].

However, crop ET_a in this study under sprinkler irrigation conditions was increased by a total of 1.8 and 4.7 mm in sprinkler irrigation I1 and I6 compared to that under non-irrigation (Figure 9E,F). This increasing trend in crop ET after sprinkler irrigation was inconsistent with the results of Zhao et al. [43] and Urrego-Pereira et al. [18]. Zhao et al. [43] ignored the evaporation of intercepted water on the canopy (the dominant component of crop ET during sprinkler irrigation [44]) and found that crop ET decreased by 1.0–1.3 mm after irrigation of 17–30 mm water compared to that under non-irrigation conditions. In the study by Urrego-Pereira et al. [18], crop ET was estimated using the Penman–Monteith method, in which the bulk canopy resistance should be effectively zero after sprinkler irrigation [45], rather than being estimated by the solar radiation-based empirical formula proposed by Farahani and Bausch [46], resulting in an 8–10% decrease in ET after sprinkler irrigation. Similar to our study, Uddin et al. [44] found that ET_a increased by 1.5 mm during and after sprinkler irrigation when the applied water was 30 mm.

On the day of sprinkler irrigation, the increased ET_a in this study was 1.1 and 1.9 mm in events I1 and I6, respectively, compared to those under non-irrigation conditions (Figure 9E,F), which accounted for 3–4% of the irrigation amount. The increased crop ET during the sprinkler irrigation period includes droplet evaporation during flight, canopy interception evaporation, and changes in crop transpiration and soil evaporation. Among these components, droplet evaporation is less than 1% of the total evaporation and can be negligible during sprinkler irrigation [47]. The water canopy interception first increases rapidly with irrigation depth, then stabilizes and reaches canopy interception capacity [48]. The canopy water interception capacity of winter wheat on the NCP ranges from 0.68 to 1.47 mm [49], and generally increases with increasing LAI and plant height [48,50]. When all of this canopy interception water is evaporated, it accounts for 62–82% of the increased ET_a on the sprinkler irrigation day. Due to the change in microclimate, the crop transpiration rate is reduced by 15–58% [12,18,51]. As a result, the increase in soil evaporation accounts for 18–38% of the increased ET_a . In the following 3–5 days after sprinkler irrigation, the daily increase in ET_a was 0.1–1.3 mm, which could be mainly due to the increase in soil evaporation when soil water at the surface layer is high. In total, one sprinkler irrigation event will cause 1.8–4.7 mm greater evapotranspiration. Given five sprinkler events in the wheat growth season, the total increased ET will be 9–24 mm, accounting for approximately 5–10% of the irrigation amount.

Owing to the increased ET_a , the K_c increased to 1.56 and 1.53 on the day of sprinkler irrigation in events I1 and I6, respectively. This K_c value was similar to that observed by Uddin et al. [19]. They found that the ratio of crop ET_a to ET_0 (namely, K_c) during sprinkler irrigation in cotton fields ranges from 1.4 at the 50% crop canopy to 1.6 at the 100% crop canopy. In this study, K_c was still higher than that before irrigation in the next few days after sprinkler irrigation (Figure 9C,D), and the duration of increased K_c was generally consistent with that of the increased ET_a and the decreased ET_0 under sprinkler irrigation. This indicates that sprinkler irrigation affects crop evapotranspiration and microclimate on the same time scale.

4.3. Microclimate Change and Related Factors in Sprinkler-Irrigated Fields

Microclimate changes were observed in this study (Figures 4–7) and have been reported in the literature [10–12,16,18,52], and these microclimate changes are of great importance for mitigating the effects of high temperature on crops [17]. Considering the great variations in these experimental conditions among studies, we developed four regression

models to separately estimate daily ΔT_{\min} , ΔT_{\max} , ΔRH and ΔVPD after sprinkler irrigation by considering the factors of irrigation amount, days after sprinkler, crop LAI, and weather and meteorological factors. Based on these four regression models, weather and meteorological factors had a great effect on field microclimate changes in the sprinkler-irrigated field (Table 5). Weather with sunny conditions showed a positive effect, while overcast weather had a negative effect. On sunny days, high R_n and air temperature and low RH always resulted in greater changes in microclimate in sprinkler-irrigated fields. Similarly, Urrego-Pereira et al. [18] demonstrated that the changes in microclimatic and maize transpiration rate are higher on drier and warmer days. Jiang et al. [11] also reported that the temperature drops 0.5 °C more at 12:00 than at 8:00 when measured at the top of the rice canopy one hour after spraying 1 mm water. In this study, the ΔT_{\min} , ΔT_{\max} , ΔVPD , and ΔRH in event I2 on a sunny day (the 3rd day after irrigation, T_{mean} , RH, and R_n were 20 °C, 59%, and 18.3 MJ m⁻² d⁻¹, respectively) were 0.6 °C, 0.6 °C, 4.2%, and 0.11 kPa higher than those on an overcast day (the 1st day after irrigation, T_{mean} , RH, and R_n were 20.6 °C, 78%, and 13.7 MJ m⁻² d⁻¹, respectively).

Higher crop LAI can cause greater canopy interception during sprinkler irrigation and higher surface cover, and finally increase water flux on the crop canopy and enhance the cooling effect [53,54]. Uddin et al. [19] reported that crop ET is the highest under full canopy crops, followed by 75% and 50% crop canopies under sprinkler irrigation conditions. In this study, under the same irrigation amount (25 mm), a larger LAI (4.8) in event I4 resulted in the maximum ΔT_{\min} (1.1 °C), ΔT_{\max} (1.0 °C), ΔVPD (0.46 kPa) and ΔRH (10.9%) compared to those (0.9 °C, 0.9 °C, 0.32 kPa, 8.9%) with a smaller LAI of 2 in event I5. The duration of microclimate change was 5–6 days in event I4, which was also longer than that (4–5 days) in event I5.

A higher irrigation amount resulted in higher ET and consequently a stronger cooling effect. Liu et al. [12] found that the daily mean air temperature within the jujube canopy from flowering to fruit set declines by 2.3, 2.6, and 3.2 °C for sprays of 2, 4 and 6 mm d⁻¹, respectively. In this study, under similar LAIs and climates, event I3, with a higher irrigation amount (37 mm), resulted in a higher maximum ΔT_{\min} (1.1 °C), ΔT_{\max} (1.3 °C), ΔRH (10.7%), and ΔVPD (0.32 kPa) and a longer microclimate change (5–7 days) than those (0.8 °C, 0.9 °C, 8.2%, 0.22 kPa, 4 days) in event I2 (21 mm).

5. Conclusions

A four-wheat-season experiment was performed to investigate the impact of sprinkler irrigation on microclimate, energy balance, and crop ET, and a novel quantitative model fitted by stepwise regression was developed to predict the change in microclimate after sprinkler irrigation. Main conclusions were as follows:

- (1) The impact of sprinkler irrigation on field microclimate lasted for 5–7 days after sprinkler irrigation with 20–50 mm water. Greater decreases in the daily minimum (0.8 °C) and maximum temperature (0.9 °C) and vapor pressure deficit (0.25 kPa) were found 1–3 days after sprinkler irrigation, after which these changes decreased and finally vanished on the 5th–7th days.
- (2) The surface reflectance rate in the sprinkler-irrigated field decreased by 0.01 in the 1–3 days after sprinkler irrigation with 40–50 mm water; the daily LE/R_n increased by 0.19–0.23, and the H/R_n decreased by 0.06–0.17.
- (3) Compared to non-irrigation conditions, the reference crop evapotranspiration decreased by 0.8–1.7 mm in 4–6 days after sprinkler irrigation, indicating lower evaporative conditions. However, crop evapotranspiration increased by 1.8–4.7 mm in a sprinkler irrigation interval, and the total increased ET was 9–24 mm when five normal sprinkler irrigations were performed in a wheat season.
- (4) Four models were developed to estimate the suppression of daily T_{\min} , T_{\max} , and VPD and the RH increase. These four indices could change more under higher irrigation amounts and sunny days with larger crop leaf area indices.

Author Contributions: Conceptualization, H.L.; investigation, X.T., L.Y., L.L. and J.C.; methodology, X.T.; writing—original draft preparation, X.T.; writing—review and editing, X.T. and H.L. All authors have read and agreed to the published version of the manuscript.

Funding: This research was funded by National Natural Science Foundation of China (NO. 51939005), National Key Research and Development Program of China (NO. 2017YFD0201500) and the 111 Project (B18006).

Institutional Review Board Statement: Not applicable.

Informed Consent Statement: Not applicable.

Data Availability Statement: Not applicable.

Acknowledgments: We thank Wenjie Zhang for his great support in the field experiments.

Conflicts of Interest: The authors declare no conflict of interest.

References

- Zaveri, E.B.; Lobell, D. The role of irrigation in changing wheat yields and heat sensitivity in India. *Nat. Commun.* **2019**, *10*, 4144. [[CrossRef](#)] [[PubMed](#)]
- Wang, X.; Müller, C.; Elliot, J.; Mueller, N.D.; Ciais, P.; Jägermeyr, J.; Gerber, J.; Dumas, P.; Wang, C.; Yang, H.; et al. Global irrigation contribution to wheat and maize yield. *Nat. Commun.* **2021**, *12*, 1235. [[CrossRef](#)] [[PubMed](#)]
- Alter, R.E.; Im, E.S.; Eltahir, E.A.B. Rainfall consistently enhanced around the Gezira Scheme in East Africa due to irrigation. *Nat. Geosci.* **2015**, *8*, 763–767. [[CrossRef](#)]
- Kang, S.; Eltahir, E.A.B. Impact of irrigation on regional climate over Eastern China. *Geophys. Res. Lett.* **2019**, *46*, 5499–5505. [[CrossRef](#)]
- Wang, W.; Liu, G.; Wei, J.; Chen, Z.; Ding, Y.; Zheng, J. The climatic effects of irrigation over the middle and lower reaches of the Yangtze River, China. *Agric. For. Meteorol.* **2021**, *308–309*, 108550. [[CrossRef](#)]
- Chen, F.; Xu, X.; Barlage, M.; Rasmussen, R.; Shen, S.; Miao, S.; Zhou, G. Memory of irrigation effects on hydroclimate and its modeling challenge. *Environ. Res. Lett.* **2018**, *13*, 064009. [[CrossRef](#)]
- Xu, L.; Shi, Z.; Wang, Y.; Chu, X.; Yu, P.; Xiong, W.; Zuo, H.; Zhang, S. Agricultural irrigation-induced climatic effects: A case study in the middle and southern Loess Plateau area, China. *Int. J. Climatol.* **2017**, *37*, 2620–2632. [[CrossRef](#)]
- Yang, Q.; Huang, X.; Tang, Q. Irrigation cooling effect on land surface temperature across China based on satellite observations. *Sci. Total Environ.* **2020**, *705*, 135984. [[CrossRef](#)]
- Mathur, R.; AchutaRao, K. A modelling exploration of the sensitivity of the India's climate to irrigation. *Clim. Dynam.* **2020**, *54*, 1851–1872. [[CrossRef](#)]
- Caravia, L.; Pagay, V.; Collins, C.; Tyerman, S.D. Application of sprinkler cooling within the bunch zone during ripening of Cabernet Sauvignon berries to reduce the impact of high temperature. *Aust. J. Grape Wine Res.* **2017**, *23*, 48–57. [[CrossRef](#)]
- Jiang, X.; Hua, M.; Yang, X.; Hu, N.; Qiu, R.; Yang, S. Impacts of mist spray on rice field micrometeorology and rice yield under heat stress condition. *Sci. Rep.* **2020**, *10*, 1579. [[CrossRef](#)] [[PubMed](#)]
- Liu, Z.; Jiao, X.; Zhu, C.; Katul, G.G.; Ma, J.; Guo, W. Micro-climatic and crop responses to micro-sprinkler irrigation. *Agric. Water Manag.* **2021**, *243*, 106498. [[CrossRef](#)]
- Issaka, Z.; Li, H.; Yue, J.; Tang, P.; Darko, R.O. Water-smart sprinkler irrigation, prerequisite to climate change adaptation: A review. *J. Water Clim. Chang.* **2018**, *9*, 383–398. [[CrossRef](#)]
- Uygan, D.; Cetin, O.; Alveroglu, V.; Sofuoğlu, A. Improvement of water saving and economic productivity based on quotation with sugar content of sugar beet using linear move sprinkler irrigation. *Agric. Water Manag.* **2021**, *255*, 106989. [[CrossRef](#)]
- International Commission on Irrigation and Drainage. Sprinkler and Micro Irrigated Area in the World. 2021. Available online: <http://www.icid.org/sprinklerandmicro> (accessed on 13 October 2021).
- Liu, H.J.; Kang, Y. Effect of sprinkler irrigation on microclimate in the winter wheat field in the North China Plain. *Agric. Water Manag.* **2006**, *84*, 3–19. [[CrossRef](#)]
- Liu, H.J.; Kang, Y. Regulating field microclimate using sprinkler misting under hot-dry windy conditions. *Biosyst. Eng.* **2006**, *95*, 349–358. [[CrossRef](#)]
- Urrego-Pereira, Y.; Caverro, J.; Medina, E.T.; Martínez-Cob, A. Microclimatic and physiological changes under a center pivot system irrigating maize. *Agric. Water Manag.* **2013**, *119*, 19–31. [[CrossRef](#)]
- Uddin, J.; Hancock, N.H.; Smith, R.J.; Foley, J.P. Measurement of evapotranspiration during sprinkler irrigation using a precision energy budget (Bowen ratio, eddy covariance) methodology. *Agric. Water Manag.* **2013**, *116*, 89–100. [[CrossRef](#)]
- National Bureau of Statistics of the People's Republic of China. *China Statistical Yearbook*; China Statistics Press: Beijing, China, 2021.
- Tang, X.; Song, N.; Chen, Z.; Wang, J.; He, J. Estimating the potential yield and ET_c of winter wheat across Huang-Huai-Hai Plain in the future with the modified DSSAT model. *Sci. Rep.* **2018**, *8*, 15370. [[CrossRef](#)]
- Yang, X.; Song, Z.; Wang, H.; Shi, Q.; Chen, F.; Chu, Q. Spatio-temporal variations of winter wheat water requirement and climatic causes in Huang-Huai-Hai Farming Region. *Chin. J. Eco-Agric.* **2012**, *20*, 356–362. [[CrossRef](#)]

23. Zhao, J.; Han, T.; Wang, C.; Jia, H.; Worqlul, A.W.; Norelli, N.; Zeng, Z.; Chu, Q. Optimizing irrigation strategies to synchronously improve the yield and water productivity of winter wheat under interannual precipitation variability in the North China Plain. *Agric. Water Manag.* **2020**, *240*, 106298. [[CrossRef](#)]
24. National Bureau of Statistics of the People's Republic of China. *China Statistical Yearbook on Environment*; China Statistics Press: Beijing, China, 2014.
25. Umair, M.; Hussain, T.; Jiang, H.; Ahmad, A.; Shen, Y. Water-saving potential of subsurface drip irrigation for winter wheat. *Sustainability* **2019**, *11*, 2978. [[CrossRef](#)]
26. Liu, H.J.; Kang, Y.; Yao, S.; Sun, Z.; Liu, S.; Wang, Q. Field evaluation on water productivity of winter wheat under sprinkler of surface irrigation in the North China Plain. *Irrig. Drain.* **2013**, *62*, 37–49. [[CrossRef](#)]
27. Ministry of Water Resources of the People's Republic of China. *Technical Standard for Microirrigation Engineering*; China Statistics Press: Beijing, China, 2020.
28. Zhang, Z.; Fei, Y. *Atlas Of groundwater Sustainable Utilization in North China Plain*; Sinomaps Press: Beijing, China, 2009.
29. The People's Government of Hebei Province. Hebei Overview. 2022. Available online: <http://www.hebei.gov.cn/hebei/14462058/14462085/14471224/index.html> (accessed on 13 October 2021).
30. GB/T 35221-2017; Specifications for Surface Meteorological Observation-General, China National Standardization Administration: Beijing, China, 2017.
31. Christiansen, J. The uniformity of application of water by sprinkler systems. *Agric. Eng.* **1941**, *22*, 89–92.
32. Liu, H.; Huang, G.; Wang, M.; Yu, L.; Ye, D.; Kang, Y.; Liu, S.; Zhang, J. Sprinkler irrigation scheme of winter wheat based on water surface evaporation of a 20 cm standard pan. *Trans. Chin. Soc. Agric. Eng.* **2010**, *26*, 11–17.
33. Teixeira, A.; Leivas, J.; Struiving, T.; Reis, J.; Simão, F. Energy balance and irrigation performance assessments in lemon orchards by applying the SAFER algorithm to Landsat 8 images. *Agric. Water Manag.* **2021**, *247*, 106725. [[CrossRef](#)]
34. Zhang, A. *Principles and Applications of Remote Sensing*; Science Press: Beijing, China, 2016.
35. Alberto, M.C.R.; Quilty, J.R.; Buresh, R.J.; Wassmann, R.; Haidar, S.; Correa, T.Q.; Sandro, J.M. Actual evapotranspiration and dual crop coefficients for dry-seeded rice and hybrid maize grown with overhead sprinkler irrigation. *Agric. Water Manag.* **2014**, *136*, 1–12. [[CrossRef](#)]
36. Zhang, Y.; Zhao, W.; He, J.; Zhang, K. Energy exchange and evapotranspiration over irrigated seed maize agroecosystems in a desert-oasis region, northwest China. *Agric. For. Meteorol.* **2016**, *223*, 48–59. [[CrossRef](#)]
37. Allen, R.G.; Pereira, L.S.; Raes, D.; Smith, M. *Crop Evapotranspiration Guidelines for Computing Crop Water Requirements-FAO Irrigation and Drainage Paper No. 56*; FAO—Food and Agriculture Organisation of the United Nations: Roma, Italy, 1998.
38. Yu, J.; Zhang, T.; Song, Z. *Mathematical Geological Method and Application*; China University of Mining and Technology Press: Xuzhou, China, 2019.
39. Lv, J.; Liu, Y.; Zhang, Z.; Dai, J. Factorial kriging and stepwise regression approach to identify environmental factors influencing spatial multi-scale variability of heavy metals in soils. *J. Hazard. Mater.* **2013**, *261*, 387–397. [[CrossRef](#)]
40. Li, P.; Ren, L. Evaluating the effects of limited irrigation on crop water productivity and reducing deep groundwater exploitation in the North China Plain using an agro-hydrological model: I. Parameter sensitivity analysis, calibration and model validation. *J. Hydrol.* **2019**, *574*, 497–516. [[CrossRef](#)]
41. Liu, H.; Liu, Y.; Zhang, L.; Zhang, Z.; Gao, Z. Quantifying extreme climatic conditions for maize production using RZWQM in Siping, Northeast China. *Int. J. Agric. Biol. Eng.* **2019**, *12*, 111–122. [[CrossRef](#)]
42. Qiu, R.; Kang, S.; Li, F.; Du, T.; Tong, L.; Wang, F.; Chen, R.; Liu, J.; Li, S. Energy partitioning and evapotranspiration of hot pepper grown in greenhouse with furrow and drip irrigation methods. *Sci. Hortic.* **2011**, *129*, 790–797. [[CrossRef](#)]
43. Zhao, W.; Li, J.; Li, Y. Modeling sprinkler efficiency with consideration of microclimate modification effects. *Agric. For. Meteorol.* **2012**, *161*, 116–122. [[CrossRef](#)]
44. Uddin, J.; Smith, R.J.; Hancock, N.H.; Foley, J.P. Evaporation and sapflow dynamics during sprinkler irrigation of cotton. *Agric. Water Manag.* **2013**, *125*, 35–45. [[CrossRef](#)]
45. Uddin, J.M.; Smith, R.J.; Hancock, N.H.; Foley, J.P. Estimation of wet canopy bulk stomatal resistance from energy flux measurements during sprinkler irrigation. *Biosyst. Eng.* **2016**, *143*, 61–67. [[CrossRef](#)]
46. Farahani, H.J.; Bausch, W.C. Performance of evapotranspiration models for maize bare soil to closed canopy. *Trans. ASAE* **1995**, *38*, 1049–1059. [[CrossRef](#)]
47. Uddin, M.J.; Murphy, S.R. Evaporation Losses and Evapotranspiration Dynamics in Overhead Sprinkler Irrigation. *J. Irrig. Drain. Eng.* **2020**, *146*, 04020023. [[CrossRef](#)]
48. Wang, Y.; Li, M.; Hui, X.; Meng, Y.; Yan, H. Alfalfa canopy water interception under low-pressure sprinklers. *Agric. Water Manag.* **2020**, *230*, 105919. [[CrossRef](#)]
49. Wang, D.; Li, J.; Rao, M. Winter wheat canopy interception under sprinkler irrigation. *Sci. Agric. Sin.* **2006**, *39*, 1859–1864.
50. Kang, Y.; Wang, Q.G.; Liu, H.J. Winter wheat canopy interception and its influence factors under sprinkler irrigation. *Agric. Water Manag.* **2005**, *74*, 189–199. [[CrossRef](#)]
51. Cavero, J.; Medina, E.T.; Puig, M.; Martínez-Cob, A. Sprinkler irrigation changes maize canopy microclimate and crop water status, transpiration, and temperature. *Agron. J.* **2009**, *101*, 854–864. [[CrossRef](#)]
52. Urrego-Pereira, Y.F.; Martínez-Cob, A.; Fernández, V.; Cavero, J. Daytime sprinkler irrigation effects on net photosynthesis of maize and alfalfa. *Agron. J.* **2013**, *105*, 1515–1528. [[CrossRef](#)]

-
53. Broadbent, A.M.; Coutts, A.M.; Tapper, N.J.; Demuzere, M. The cooling effect of irrigation on urban microclimate during heatwave conditions. *Urban Clim.* **2018**, *23*, 309–329. [[CrossRef](#)]
 54. Li, B.; Shi, B.; Yao, Z.; Shukla, M.; Du, T. Energy partitioning and microclimate of solar greenhouse under drip and furrow irrigation systems. *Agric. Water Manag.* **2020**, *234*, 106096. [[CrossRef](#)]